The Effects of Pt Doping on the Photo-reactivity of TiO$_2$

D D Sahoo[1], G S Roy[2*]

1.   Mahanga puspagiri Mahavidyalaya, Erakana, Cuttack,Odisha
2.   Chairman CHSE, Bhubaneswar, Odisha
gsroy2004@gmail.com

Abstract: Titanium dioxide (TiO$_2$), which is doped with platinum metal ions (Pt^{4+}, Pt^{2+}), is synthesized by standard sol-gel methods and characterized by X-ray diffraction (XRD) and UV-Vis diffuse reflectance spectroscopy. Doping with Pt(IV.II), resulted in a lower anatase to rutile phase transformation temperature for the resultant TiO$_2$ particles, Metal-ion doping also resulted in a red-shift of the photophysical response of TiO$_2$ that was reflected in an extended absorption in the visible between 400 and 700 nm.

Keywords: XRD, UV-Vis Spectra, Doping

Introduction

Semiconductor photocatalysis has received much attention during last three decades as a promising solution for both energy generation and environmental problems. Since the discovering of Fujishima and Honda[1] that water can be photo-electrochemically decomposed into hydrogen and oxygen using a semiconductor (TiO$_2$) electrode under UV irradiation, extensive works have been carried out to produce hydrogen from water splitting using a variety of semiconductor photocatalysts. In recent years, scientific and engineering interest in heterogeneous photocatalysis has been also focused on environmental applications such as water treatment and air purification. Many review papers on semiconductor photocatalysis can be found in literature[1-6]. Semiconductor photocatalysis is initiated by electron-hole pairs after bandgap excitation. When a photocatalyst is illuminated by light with energy equal to or greater than band-gap energy, the valence band electrons can be excited to the conduction band, leaving a positive hole in the valence band:

Photocatalyst (e.g., TiO$_2$) $\rightarrow$ e$_{CB}^-$ + h$_{VB}^+$ (1.1)
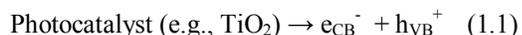
The excited electron-hole pairs can recombine, releasing the input energy as heat, with no chemical effect. However, if the electrons (and holes) migrate to the surface of the semiconductor without recombination, they can participate in various oxidation and reduction reactions with adsorbed species such as water, oxygen, and other organic or inorganic species[7-10]. These oxidation and reduction reactions are the basic mechanisms of photocatalytic water/air remediation and photocatalytic hydrogen production, respectively. A simplified mechanism for photocatalytic process on a semiconductor is presented in Figure 1.
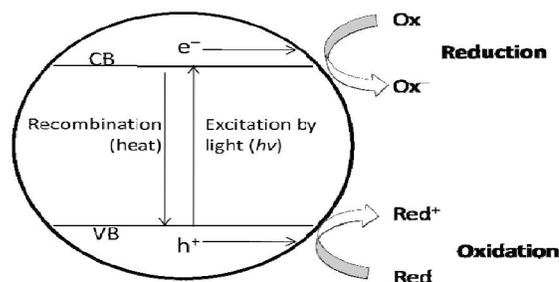

Figure 1 - Simplified mechanism of semiconductor photocatalytic process

For photocatalytic water/air remediation as an environmental application, valence band (VB) holes are the important elements that induce the oxidative decomposition of environmental pollutants. The positive hole can oxidize pollutants directly, but mostly they react with water (i.e., hydroxide ion, OH–) to produce the hydroxyl radical (•OH), which is the very powerful oxidant with the oxidation potential of 2.8 V (NHE). •OH rapidly attacks pollutants at the surface and in solution as well and can mineralize them into CO$_2$, H$_2$O, etc. TiO$_2$, the most popular photocatalyst because of its relatively high activity, chemical stability, availability with low production costs, and non-toxicity has been widely studied and proven to have a potential to completely oxidize a variety of organic compounds, including persistent organic pollutants. The reducing conduction band (CB) electrons are more important when photocatalytic reaction is applied for hydrogen production from water splitting. In order to initiate hydrogen production, the conduction band level must be more negative than the hydrogen production level:

$$2H_2O \rightarrow 2H_2 + O_2 \qquad (1.2)$$
$$H_2O \leftrightarrow H^+ + OH^- \qquad (1.3)$$
$$2H_2O + 2e^- \rightarrow H_2 + 2OH^- \qquad (1.4)$$
$$2H_2O \rightarrow O_2 + 4H^+ + 4e^- \qquad (1.5)$$

The redox potential for overall reaction (eq. 1.2) at pH 7 is EH = -1.23 V (NHE), with the corresponding half-reactions of -0.41 V (eq 1.4) and 0.82 V (eq 1.5), which gives a ΔG^o = +237 kJ/mole).[7] A large number of metal oxides and sulfides have been examined as photocatalysts for hydrogen production and environmental application. The majority of the simple metal oxide photocatalysts, however, are primarily active under UV. For example, TiO_2 has a wide band-gap energy of 3.0 ~ 3.2 eV which prevents the utilization of visible-light that accounts for most of solar energy. More recently, significant efforts have also been made to develop new or modified semiconductor photocatalysts that are capable of using visible-light including metal ion doping, nonmetallic element doping, and sensitization with organic dyes or small band-gap semiconductors such as CdS. Metal ion doping has been primarily studied to enhance the photocatalytic activity under UV irradiation. In recent years, however, extensive research works have focused on visible-light induced photocatalysis by metal ion-doped semiconductor, since some of these have shown the extended absorption spectra into visible-light region. This property has been explained by the excitation of electrons of dopant ion to the conduction band of semiconductor (i.e., a metal to conduction band charge-transfer). Numerous metal ions, including transition metal ions (e.g., vanadium, chromium, iron, nickel, cobalt, ruthenium and platinum) and rare earth metal ions (e.g., lanthanum, cerium, and ytterbium), have been investigated as potential dopants for visible-light induced photocatalysis. However, metal ion dopant can also serve as a recombination center, resulting in decreased photocatalytic activities. Unlike metal ion doping, nonmetallic dopants replace lattice oxygen and are less likely form recombination centers. Sensitization methods are widely used to utilize visible-light for energy conversion. In case of sensitization with organic dyes, dye molecule electrons excited by visible light can be injected to the CB of semiconductor to initiate the catalytic reactions as shown in Figure 2(a). Similarly, sensitization with a small band-gap semiconductor is made by coupling a large band-bap semiconductor with a small band-gap semiconductor with a more negative conduction level (i.e., hybrid or composite photocatalyst). In composite photocatalyst, the CB electrons photo-generated from a small band-gap semiconductor by the absorption of visible-light can

be injected to the CB of a large band gap semiconductor, while the photo-generated holes are trapped in a small band-gap semiconductor. Thus, an effective electron-hole separation can be achieved, as shown in Figure 1.2(b). CdS with band-gap energy of 2.4 eV has been frequently used to form hybrid or composite photocatalysts. In this work we have synthesized the TiO_2 through sol-gel synthesis process and after that we have doped the metal ion to get the photocatalysed behavior.
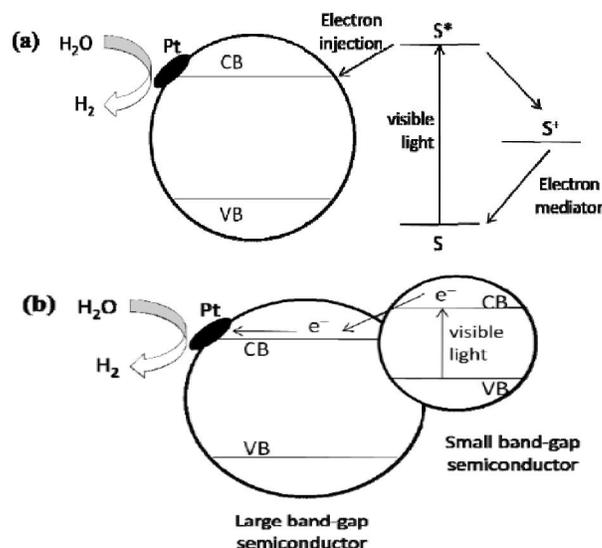

Figure 2: Schematic diagram of visible-light induced photocatalysis with sensitizations: (a) sensitization with organic dyes and (b) sensitization with small band-gap semiconductor

Preparation of Pt doped TiO_2

Titanium (IV) tetrabutoxide was hydrolyzed with deionized water (100ml). And the resulting titanium hydroxide precipitate was separated by decantation and washed thoroughly with water 2-3 times to remove alcohol generated during hydrolysis of titanium alkoxide. The precipitate was dissolved in 75 ml of aqueous hydrogen peroxide to get a transparent orange sol of Ti-peroxo complex. peroxo complex was diluted with water to obtain the solution of different concentrations and the Color of the sol changes from brick red to yellow after dilution. For doping various transition metal ions, salt of metal ions were dissolved in water and the resultant solution was added drop wise into the TiO2 precursor sol. Here we have doped the Pt^{4+} with TiO_2.

Results and Discussion

The structure of TiO_2 samples synthesized by standard sol-gel methods appeared to be

amorphous thermal annealing; however, post-synthesis treatment at various temperatures ranging from 200 to 700 °C resulted in higher degree crystallinity primarily as anatase. The increasing calcination temperatures resulted in an increase in the intensity and sharpness of the anatase peaks. This trend is clearly indicative of an improvement in the degree of crystallinity corresponding to the formation of larger particles with fewer defects. However, above a given temperature XRD peaks corresponding to the rutile phase appear. However, it is conceivable that metal impurities, which were formed during synthesis, were nanoscopic or possibly dispersed on the surface. We have assumed that some of the metal ion dopants such as Pt^{4+} ions are most likely to be substituted at Ti^{4+} sites within TiO_2 because ionic radii of dopants are similar to that of Ti^{4+}, whereas some other metal dopants such as Pt^{2+} ions are possibly located in interstitial positions of the lattice rather than directly in Ti^{4+} sites because of the relatively large size difference between dopant ions and Ti^{4+}. Thus, they are more likely to be found as dispersed metal oxides within the crystal matrix or they are dispersed on the surface of TiO_2.
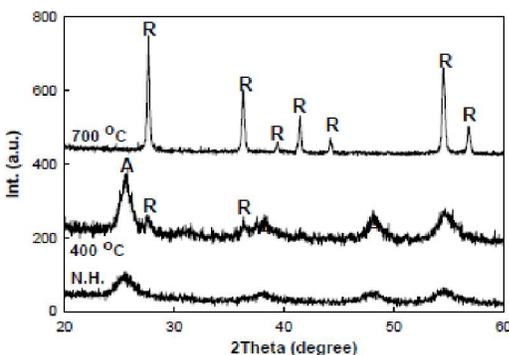

Figure 3: XRD of Pt-TiO_2

The anatase-to-rutile phase transformation (i.e., the A-R phase transformation) of pure TiO_2 normally occurs between 600 and 700 °C. In our case, pure (undoped) TiO_2 samples that were calcined at 400 °C showed only the anatase phase. Calcination at 700 °C produced with a relatively small fraction of the rutile phase. However, it was observed that, in some cases, Pt-ion doping altered the temperature of the A-R phase transformation of TiO_2. In this regard, the XRD patterns of representative Pt-TiO_2 samples that was calcined at different temperatures are shown in Figure 3. Similar to undoped TiO_2. In the case of Pt-TiO_2, a rutile peak at $2\theta = 27.5^o$ appeared at 400 °C. This rutile peak was clearly dominant at 700 °C,

while the anatase peak at $2\theta = 25.7^o$ disappeared at 700 °C.

UV-Vis Diffuse Reflectance Spectroscopy

The UV-Vis diffuse reflectance spectra of the array of Pt^{4+} ion-doped TiO_2 samples are shown in Figure 4. The sol-gel synthesized, undoped TiO_2 is characterized by sharp absorption edges at about 400 nm (Ebg ~ 3.1 eV) However, most of Pt-TiO_2 samples show extended absorption spectra into visible region in the range of 400 ~ 700 nm which illustrates the difference between the absorption spectra of Pt(IV)-TiO_2 and Pt(II)-TiO_2. Pt(II)-TiO_2 shows a much broader absorption over most of the visible region. However, Pt(IV)-TiO_2 has a smaller absorption peak between 400 and 550 nm.
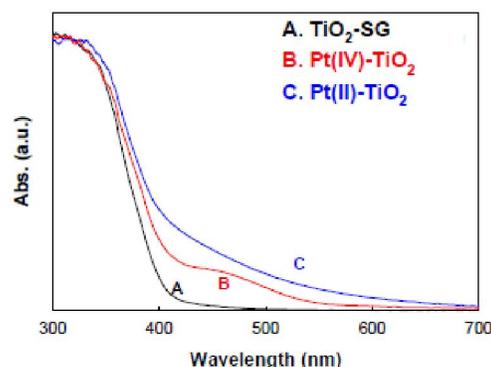

Figure 4: UV-Vis diffuse reflectance spectra of Pt-TiO_2

Conclusion

In conclusion, we have synthesized an array of platinum doped titanium dioxide materials, in order to evaluate their visible-light photocatalytic activities. Pt-TiO_2 lowered the temperature of the anatase-to-rutile phase transformation. However, there appears to be no correlation between the effectiveness of an individual dopant on the A-R phase transformation and its valence state or ionic radius Pt-TiO_2 which was prepared at a 0.3 % doping level and annealed at 400 °C, had a relatively high fraction of rutile and showed significantly enhanced photocatalytic activity compared to SG-TiO_2 for all test reactions under visible-light irradiation. These results indicate that the presence of the rutile structure in the doped TiO_2 may affect photocatalytic activities of Pt-TiO_2 .

References

1. Hoffmann, M. R.; Martin, S. T.; Choi, W. Y.; Bahnemann, D. W. Chem. Rev.1995, 95, 69.
2. Linsebigler, A. L.; Lu, G. Q.; Yates, J. T. Chem. Rev. 1995, 95, 735.
3. Mills, A.; LeHunte, S. J. Photochem. Photobiol. A 1997, 108, 1.
4. Zhao, J.; Yang, X. D. Building and Environment 2003, 38, 645.
5. Bahnemann, D. Sol. Energ. 2004, 77, 445.
6. Kudo, A.; Kato, H.; Tsuji, I. Chem. Lett. 2004, 33, 1534.
7. Asahi, R.; Morikawa, T.; Ohwaki, T.; Aoki, K.; Taga, Y. *Science* **2001**, *293*, 269.
8. Batzill, M.; Morales, E. H.; Diebold, U. *Phys. Rev. Lett.* **2006**, *96*.
9. Livraghi, S.; Paganini, M. C.; Giamello, E.; Selloni, A.; Di Valentin, C.; Pacchioni, G. *J. Am. Chem. Soc.* **2006**, *128*, 15666.

12/27/2012